NeuroImage: Clinical 19 (2018) 507–515

Contents lists available at ScienceDirect

NeuroImage: Clinical

journal homepage: www.elsevier.com/locate/ynicl

Information processing speed in multiple sclerosis: Relevance of default mode network dynamics

Q. van Geest[a,*], L. Douw[a,b], S. van 't Klooster[a], C.E. Leurs[c], H.M. Genova[d,e], G.R. Wylie[d,e], M.D. Steenwijk[a], J. Killestein[c], J.J.G. Geurts[a], H.E. Hulst[a]

[a] Department of Anatomy & Neurosciences, Neuroscience Amsterdam, VUmc MS Center Amsterdam, VU University Medical Center, Amsterdam, The Netherlands
[b] Department of Radiology, Athinoula A. Martinos Center for Biomedical Imaging, Massachusetts General Hospital, Charlestown, MA, USA
[c] Department of Neurology, Neuroscience Amsterdam, VUmc MS Center Amsterdam, VU University Medical Center, Amsterdam, The Netherlands
[d] Neuropsychology and Neuroscience Laboratory, Kessler Foundation, West Orange, NJ, USA
[e] Department of Physical Medicine and Rehabilitation, Rutgers New Jersey Medical School, Newark, NJ, USA

ARTICLE INFO

Keywords:
Dynamic functional connectivity
Functional connectivity
Information processing speed
Default mode network
Cognition
Multiple sclerosis

ABSTRACT

Objective: To explore the added value of dynamic functional connectivity (dFC) of the default mode network (DMN) during resting-state (RS), during an information processing speed (IPS) task, and the within-subject difference between these conditions, on top of conventional brain measures in explaining IPS in people with multiple sclerosis (pwMS).

Methods: In 29 pwMS and 18 healthy controls, IPS was assessed with the Letter Digit Substitution Test and Stroop Card I and combined into an IPS-composite score. White matter (WM), grey matter (GM) and lesion volume were measured using 3 T MRI. WM integrity was assessed with diffusion tensor imaging. During RS and task-state fMRI (i.e. symbol digit modalities task, IPS), stationary functional connectivity (sFC; average connectivity over the entire time series) and dFC (variation in connectivity using a sliding window approach) of the DMN was calculated, as well as the difference between both conditions (i.e. task-state *minus* RS; ΔsFC-DMN and ΔdFC-DMN). Regression analysis was performed to determine the most important predictors for IPS.

Results: Compared to controls, pwMS performed worse on IPS-composite ($p = 0.022$), had lower GM volume ($p < 0.05$) and WM integrity ($p < 0.001$), but no alterations in sFC and dFC at the group level. In pwMS, 52% of variance in IPS-composite could be predicted by cortical volume ($\beta = 0.49$, $p = 0.01$) and ΔdFC-DMN ($\beta = 0.52$, $p < 0.01$). After adding dFC of the DMN to the model, the explained variance in IPS increased with 26% ($p < 0.01$).

Conclusion: On top of conventional brain measures, dFC from RS to task-state explains additional variance in IPS. This highlights the potential importance of the DMN to adapt upon cognitive demands to maintain intact IPS in pwMS.

1. Introduction

Up to 50% of people with multiple sclerosis (pwMS) suffer from problems with information processing speed (IPS), also known as "cognitive slowing". Deficits in IPS are among the first cognitive symptoms in pwMS and related to reduced quality of life (Chiaravalloti and DeLuca, 2008; Benedict et al., 2006; Amato et al., 2010; Glanz et al., 2010). The search for neural correlates of IPS deficits resulted in several structural and functional brain measures. These include white and grey matter damage (e.g. lesions, atrophy and reduced tissue integrity) (Randolph et al., 2005; Mazerolle et al., 2013; Batista et al., 2012), but also changes in activation and functional connectivity (FC) during an IPS task or during resting-state (RS) (Genova et al., 2009; Dobryakova et al., 2016; Wojtowicz et al., 2014). Although these measures do explain IPS to a certain extent, there is still room to improve the relationship between brain measures and IPS. For example, intuitively IPS depends on the ability of the brain to rapidly transfer information within its functional network. As FC measures have previously been averaged over the entire scanning session (i.e. time series), from here on referred to as *stationary FC* (sFC), the *variability* in FC over time has not been taken into account. With this latter measure, the *changes* in connectivity strength *during* a time series are obtained, from here on referred to as *dynamic* FC (dFC). As dFC seems to be behaviorally relevant with respect to cognition in healthy subjects (Cohen,

* Corresponding author.
E-mail address: q.vangeest@vumc.nl (Q. van Geest).

https://doi.org/10.1016/j.nicl.2018.05.015
Received 20 March 2018; Received in revised form 30 April 2018; Accepted 13 May 2018
Available online 15 May 2018

2017; Jia et al., 2014; Gonzalez-Castillo and Bandettini, 2017) or symptoms in neurological disorders (Zhang et al., 2016; Sambataro et al., 2017; Douw et al., 2015), we argue that dFC could also be of importance for maintained IPS in pwMS, as it could reflect the fast changing connectivity patterns within the brain that cannot be captured with sFC (Cohen, 2017).

1.1. Brain networks

The brain's functional network has an *intrinsic* organization, namely various (interconnected) RS networks that can be identified with RS functional magnetic resonance imaging (fMRI). This intrinsic organization of the brain has been linked to cognitive functioning, as it is thought enable the flow of activity (i.e. information) during task performance (Cole et al., 2016; Ito et al., 2017). An important brain network related to cognitive (dys)functioning is the default mode network (DMN) (Raichle, 2015). This network consists of several core regions, including the medial temporal lobe, medial prefrontal cortex, posterior cingulate cortex, and inferior parietal cortex (Raichle, 2015). Recent studies have shown task-related "responsivity" in sFC of the DMN, that is, the ability to change the connection strength upon task demands, to enable information integration throughout the brain (Elton and Gao, 2015; Vatansever et al., 2015a).

1.2. Dynamics of the DMN

Previous studies have linked DMN dynamics during RS or task-state to cognitive functioning, such as executive functioning, cognitive flexibility, concept formation, and (working) memory, in healthy subjects and individuals with neurological disorders (e.g. temporal lobe epilepsy and MS) (Douw et al., 2015; Liu et al., 2018; Douw et al., 2016; Simony et al., 2016; Vatansever et al., 2015b; Yang et al., 2014; Nomi et al., 2017; van Geest et al., 2018). Furthermore, one study in healthy subjects showed that a larger increase in dFC between the DMN and frontoparietal network during task-state relative to RS was related to better cognitive flexibility outside the scanner (i.e. Stroop task) (Douw et al., 2016). Together with studies showing differences in dFC between RS and task-state, the change in dFC of the DMN between RS and task-state might reflect the ability of the brain to adapt as task demands change, in order to optimally execute the task at hand (i.e. increased information processing throughout the brain) (Cohen, 2017; Braun et al., 2015; Lin et al., 2017; Xie et al., 2017).

To investigate whether dFC of the DMN is indeed a neural correlate of IPS in MS, and relevant next to previously identified correlates, we explored its incremental value when explaining IPS variance on top of conventional measures of brain abnormalities (defined as: brain atrophy, lesions, white matter integrity, and sFC of the DMN). We hypothesized that dFC of the DMN, and especially the *difference* in dFC between RS and task-state, that is, the ability of the brain to adapt upon task demands, would explain unique variance in IPS.

2. Materials and methods

2.1. Subjects and study design

In this prospective observational study, all pwMS ($N = 33$) and healthy controls (HCs; $N = 19$) met the following inclusion criteria: 1) aged 18–65 years; 2) no contra-indications for MRI; 3) no psychiatric or neurological disease (for pwMS: other than MS). For pwMS, additional inclusion criteria were: 4) a diagnosis of relapsing-remitting MS, and; 5) without relapse or steroid treatment for at least four weeks prior to study measurements. Subjects performing below chance level (< 50% correct, $n = 3$ pwMS) on the fMRI paradigm were excluded from the entire study, as well as subjects with many frame-to-frame head displacements (> 0.5 mm for > 20% of frames, $n = 1$ pwMS and $n = 1$ HC) during fMRI to minimize motion effects on dFC measures (Shine et al., 2016). The study was approved by the local institutional ethics review board and conducted in accordance with the ethical standards laid down in the Declaration of Helsinki. All subjects gave written informed consent.

This study is part of a study investigating the effect of fingolimod on the brain and cognitive functions over a period of 1.5 years. Here, the baseline data are presented (no prior publications on this dataset). The final MS group consisted of pwMS switching from first-line treatment ($n = 7$) or natalizumab ($n = 6$) to fingolimod treatment (from here on referred to as *switchers*), and pwMS continuing first-line therapy ($n = 16$; from here on referred to as *non-switchers*). The MS group and HCs were matched for age, sex, educational level, and disease duration for pwMS only.

2.2. Clinical measures

All subjects underwent neuropsychological testing, including, among others, the Letter Digit Substitution Task (LDST; oral version, 90 s), which is an equivalent of the Symbol Digit Modalities Test (SDMT) (Jolles et al., 1995), and the Stroop Test (for all tests see Appendix) (De, 1973). Scores on all neuropsychological tests were converted into a *Z*-score relative to HCs. Scores on the LDST and Stroop Card 1 were averaged into one IPS composite *Z*-score. Anxiety and depression levels were assessed with the Hospital Anxiety and Depression Scale (Zigmond and Snaith, 1983). Fatigue was measured using the Checklist of Individual Strength (Vercoulen et al., 1994). Additionally, physical disability was assessed by a trained physician using the Expanded Disability Status Scale (EDSS) (Kurtzke, 1983).

2.3. MRI acquisition

All subjects were examined using a 3 T whole-body MRI scanner (GE Signa-HDxt, Milwaukee, WI, USA) with a 32-channel head coil. The protocol included the following sequences: three-dimensional (3D) T1-weighted fast spoiled gradient echo for volume measurements (repetition time (TR): 8.22 ms; echo time (TE): 3.22 ms; inversion time (TI): 450 ms; flip angle 12°; 1.0 mm sagittal slices; 0.94 × 0.94 mm^2 in-plane resolution); 3D fluid-attenuated inversion recovery (FLAIR; TR: 8000 ms; TE: 128 ms; TI: 2343 ms; 1.2 mm sagittal slices; 0.98 × 0.98 mm^2 in-plane resolution) for white matter (WM) lesion detection; and diffusion tensor imaging (DTI; TR: 7200 ms; TE: 83 ms; flip angle 90°; 57 axial slices with an isotropic 2.0 mm resolution) with 5 volumes without directional weighting and 30 volumes with non-collinear diffusion gradients (b-value: 1000 s/mm^2) to assess WM integrity. To correct for echo planar imaging (EPI) induced artifacts, two scans with reversed phase-encode blips were acquired for DTI. Furthermore, RS fMRI (eyes closed; EPI, 202 volumes, TR: 2200 ms; TE: 35 ms; flip angle 80 degrees; 3 mm contiguous axial slices; 3.3 × 3.3 mm^2 in-plane resolution) and task-related (i.e. task-state) fMRI (IPS paradigm; EPI, 460 volumes, TR: 2000 ms; TE: 30 ms; flip angle 80 degrees; 4 mm contiguous axial slices; 3.3 × 3.3 mm^2 in-plane resolution) were performed to measure sFC and dFC.

2.4. Structural MRI measures

2.4.1. Whole-brain and lesion volume

Lesions were automatically segmented on FLAIR images and filled on the 3DT1 images using LEAP (Steenwijk et al., 2013; Chard et al., 2010). WM and grey matter (GM) volumes were measured using SIENAX (Smith et al., 2002). Volumes of deep GM structures were measured using FIRST (FSL v5.0.9, fmrib.ox.ac.uk/fsl). Cortical GM volume was measured by subtracting the FIRST segmentation from SIENAX's GM segmentation. All volumes were normalized for head size using the v-scaling factor obtained by SIENAX, resulting in normalized WM volume (NWMV), normalized cortical GM volume (NCGMV), normalized deep GM volume (NDGMV), and normalized lesion volume (NLV).

2.4.2. Severity and extent of WM damage

The susceptibility-induced off-resonance field was estimated for the diffusion weighted sequence using a method described previously, and the two images were combined into a single corrected one (and used for further processing) (Andersson et al., 2003). Motion- and eddy-current correction was performed, followed by diffusion tensor fitting (FMRIB's Diffusion Toolbox, FSL, http://www.fmrib.ox.ac.uk/fsl). Tract-based spatial statistics with default settings was used to obtain skeletonized fractional anisotropy (FA) maps (Smith et al., 2006). In order to obtain individual measures of whole-brain WM integrity damage, we quantified the *severity* and *extent* of WM damage using a method that has been described previously (Schoonheim et al., 2014). In short, each subject's skeleton was voxelwise expressed as a *Z*-score relative to HCs. The *severity* of WM damage in a subject was subsequently calculated by computing average normalized FA score within the skeleton. The *extent* of WM damage was calculated by counting the number of voxels exceeding the threshold of $Z < -3.1$ ($p < 0.001$) in each subject (Schoonheim et al., 2014). Finally, the whole-brain average FA of the white matter was obtained for each subject.

2.5. Functional MRI

2.5.1. Task-state fMRI paradigm

Task-state fMRI was obtained by examining IPS using the modified version of the SDMT (mSDMT) inside the scanner (Genova et al., 2009). Briefly, in the stimulus condition a panel of nine paired stimulus boxes were presented. The boxes in the upper row contained a symbol, while the boxes in the lower row contained a digit (1 to 9). Below this panel, a symbol-digit pair was presented and the subject had to indicate via a button box whether or not this symbol-digit pair matched one of the pairs in the upper panel. The timing of the stimuli was pre-specified. Accuracy was used for the analyses of behavioral task data. Reaction time for correct trials was not included, as this can be influenced by motor problems in pwMS. The paradigm lasted approximately 15 min.

2.5.2. Preprocessing of fMRI data

Preprocessing of RS and task-state functional images was performed separately with MELODIC (FSL), and consisted of: 1) discarding the first five volumes; 2) high-pass filtering (1 s cutoff); 3) mcFlirt motion correction, and; 4) spatial smoothing (6 mm full width-at-half-maximum Gaussian kernel). Distortion correction on the functional images was not performed. Motion parameters were obtained and the processed functional images were subsequently nonlinearly registered to Montreal Neurological Institute standard space by using the individuals 3D T1 weighted image. Quality control consisted of checking for excessive head motion and visual inspection of all processed images and registration steps.

2.5.3. Atlas construction

In this study, we used the Brainnetome atlas (Fan et al., 2016) (210 regions) to parcellate the brain. By overlaying the Yeo7 RS network atlas (Yeo et al., 2011) on the Brainnetome atlas, we were able to identify which Brainnetome regions belonged to the DMN based on two criteria: 1) > 50% of voxels of a Brainnetome region had to overlap with the DMN from the Yeo7 atlas, and 2) the overlap with the DMN should be the highest and the differences in overlap with the second highest RS network should be > 15%. In total, 38 regions of the Brainnetome atlas were considered part of the DMN. After preprocessing of RS and task-state images, the Brainnetome atlas in standard space was non-linearly registered to each subject's 3DT1 image, and subsequently masked for GM (binarized SIENAX segmentation). Next, the subcortical regions derived by FIRST were added, resulting in an atlas containing 224 regions. This novel atlas was then linearly registered to RS and task-state fMRI space, where areas known to be prone to artifacts were removed (e.g. orbitofrontal cortex), by excluding voxels with a signal intensity in the lowest quartile of the robust intensity range (i.e. the minimum and maximum if the outer tails of the intensity distribution are ignored). Finally, the average time series for each brain region was obtained during RS and task-state fMRI, and imported into Matlab R2012a (Natick, Massachusetts, USA) for further analysis.

2.5.4. Stationary FC

To obtain sFC, Pearson correlation coefficients between all brain regions (i.e. region of interest-wise analysis) over the entire time series (absolute values) were calculated for RS and task-state fMRI separately (see Fig. 1A).

2.5.5. Dynamic FC

For dFC, a sliding-window approach was used with settings that were selected based on previous studies (see Fig. 1A), resulting in 35 and 86 sliding windows for RS and task-state time series, respectively (van Geest et al., 2018; Leonardi and Van De Ville, 2015). For RS time series the window length was 27 volumes (59.4 s) with a shift of 5 volumes (11 s). For task-state time series, the window length was 30 volumes (60 s) with a shift of 5 volumes (10 s). Note that the differences in window length and shift were caused by differences in TR. Then, absolute Pearson correlation coefficient was calculated between all 224 regions for each window. Next, the absolute difference in FC was calculated between each consecutive window and subsequently summed per matrix cell, resulting in a 224 by 224 dFC matrix.

2.5.6. DMN connections

For RS and task-state, sFC and dFC was averaged over all DMN regions. Concretely, this resulted in an average of both within-DMN and DMN-to-whole-brain connectivity. To correct for the difference in the number of fMRI volumes between both conditions, and to be more specific to detect regional changes, each sFC and dFC measure was divided by its corresponding whole-brain average sFC and dFC. Furthermore, we calculated the *difference* in sFC of the DMN (ΔsFC-DMN) between RS and task-state as follows: task-state sFC DMN – RS sFC DMN. The differences in dFC of the DMN (ΔdFC-DMN) was calculated similarly: task-state dFC DMN – RS dFC DMN. Positive values indicate an *increase* in sFC or dFC in task-state relative to RS. See Fig. 1B and C for a schematic overview of functional measures.

2.6. Statistical analysis

Statistical analyses were performed in SPSS version 22 (Armonk, NY, USA). Normality of variables was investigated using the Kolmogorov-Smirnov test and visual inspection of histograms. NLV and the extent of WM damage were log-transformed to obtain normally distributed data. EDSS, educational level, questionnaires for anxiety and depression, and mSDMT accuracy were not transformed and tested with Mann-Whitney *U* tests. Univariate and multivariate general linear models were constructed to assess group differences in behavioral measures (IPS, questionnaires, task performance), structural MRI (atrophy, extent and severity of white matter damage), sFC, and dFC (with average head motion as covariate to further limit its effect on the analyses). We performed a two-tailed one-sample *t*-test in each group to test whether ΔsFC-DMN and ΔdFC-DMN differed from zero (indicating a change). The differences in ΔsFC-DMN and ΔdFC-DMN *between* groups were analyzed with a univariate general linear model. Additionally, we explored the relationship between dFC and conventional brain measures using Pearson correlation coefficients. Because of multiple testing regarding brain measures and the correlation analyses, Benjamini-Hochberg false discovery rate corrected *p*-values (corr. *p*) are reported for these analyses (Benjamini and Hochberg, 1995).

Hierarchical regression analysis with a forward feature selection scheme was performed to investigate the incremental value of dFC of the DMN over conventional brain measures in explaining mSDMT accuracy and IPS outside the scanner. The following blocks were included: block 1 (confounders): age, sex, education; block 2: NWMV,

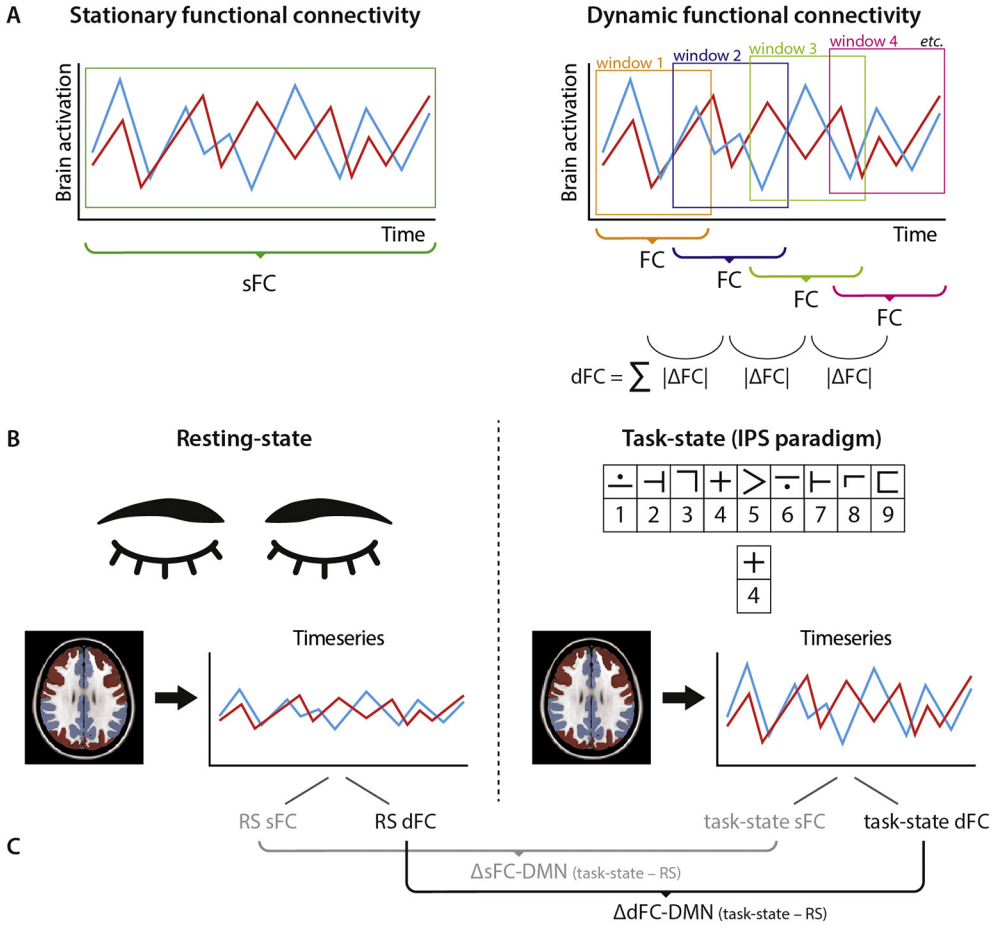

Fig. 1. Schematic overview of functional measures

Stationary (s) functional connectivity (FC) was calculated with Pearson correlation coefficients over the entire time series, whereas for dynamic (d) FC the time series were divided into sliding windows (A). For each sliding window, FC was calculated and subsequently the absolute difference between each consecutive window was calculated and summed as a measure of dFC. For both resting-state (RS) and task-state fMRI, sFC and dFC of the default mode network was obtained (B). Additionally, the difference in sFC and dFC between task-state and RS was calculated (C). dFC = dynamic functional connectivity; FC = functional connectivity; IPS = information processing speed; RS = resting-state; sFC = stationary functional connectivity; ΔdFC-DMN = difference in dynamic functional connectivity between task-state and resting-state (task-state minus resting-state); ΔdFC-DMN = difference in stationary functional connectivity between task-state and resting-state (task-state minus resting-state).

NCGMV, NDGMV, NLV; block 3: FA extent, FA severity; block 4: RS sFC DMN, task-state sFC DMN, ΔsFC-DMN; block 5: RS dFC DMN, task-state dFC DMN, ΔdFC-DMN. Post hoc, we explored the effect of switching medication on IPS and its possible moderating effects on the significant predictors for IPS. In order to do so, we performed regression analyses with mSDMT accuracy or IPS composite *Z*-score as dependent variable, and included the significant predictors obtained by the main regression analysis as independent variables together with a variable coding for switchers/non-switchers in block 1 (enter method). In block 2, we entered the interaction effects between switchers/non-switchers and predictors defined in block 1. *p*-values lower than 0.05 were considered as statistically significant.

2.6.1. Post hoc specificity analysis

To investigate the specificity of the relationship between dynamic brain measures that were significantly related to IPS, we performed a correlation analysis (Spearman's rank correlation) with other outcome variables, including EDSS score, fatigue, depression, and all neuropsychological tests.

3. Results

3.1. Demographics and clinical measures

The final sample size included 29 pwMS (18 women; mean age: 41.3 ± 9.3 years; mean disease duration 11.1 ± 7.1 years) and 18 HCs (11 women; mean age: 40.7 ± 13.3 years; see Table 1). No differences between groups were found for age, sex, and educational level. Anxiety and depression scores were similar between groups, but pwMS reported more fatigue than controls (pwMS: 72.0 ± 33.6; HCs: 47.1 ± 18.3; $p = 0.007$). Compared to HCs, pwMS performed worse on the LDST (*Z*-score: −1.1 ± 1.4; $p = 0.005$), but not on the Stroop Card 1 (*Z*-score: −0.5 ± 1.4; $p = 0.186$). The IPS composite *Z*-score was lower in pwMS (*Z*-score: −0.8 ± 1.3) compared to HCs (*Z*-score: 0.0 ± 0.8; $p = 0.022$). Furthermore, compared to HCs, pwMS performed worse on tests for visuospatial memory, executive functioning,

Table 1
Demographics and clinical measures.

	pwMS ($n = 29$)	HCs ($n = 18$)	p
Age	41.25 (9.34)	40.68 (13.29)	0.863
Sex (female/male)	18/11	11/7	0.948
Educational level[a]	6.00 (5.00–7.00)	6.00 (5.00–7.00)	0.098
Disease duration	11.05 (7.11)	–	–
EDSS[a]	3.00 (1.00–6.00)	–	–
HADS-A[a]	5.50 (0.00–12.00)[b]	4.00 (2.00–13.00)	0.170
HADS-D[a]	3.00 (0.00–14.00)[b]	1.50 (0.00–6.00)	0.229
CIS20r	71.97 (33.58)[b]	47.06 (18.29)	0.007
Z-score LDST	−1.11 (1.38)	0.00 (1.00)	0.005
Z-score Stroop Card 1	−0.51 (1.41)	0.00 (1.00)	0.186
IPS composite *Z*-score	−0.81 (1.31)	0.00 (0.78)	0.022
mSDMT performance (inside scanner)			
Accuracy (%)[a]	95.45 (77.27–100.00)	96.36 (86.36–100.00)	0.307

Displayed data are mean (standard deviation).
CIS20r = Checklist of Individual Strength – revised; EDSS = Expanded Disability Status Scale; HCs = healthy controls; HADS = Hospital Anxiety and Depression Scale; A = Anxiety; D = Depression; IPS = information processing speed; LDST = Letter Digit Substitution Test; mSDMT = modified Symbol Digit Modalities Test; pwMS = people with multiple sclerosis.

[a] Displayed data are median (minimum – maximum).

[b] $n = 28$.

Table 2
Brain volumes and white matter damage.

	pwMS (n = 29)	HCs (n = 18)	Effect size (η^2)	p	p corr.
NWMV, ml	682.55 (46.91)	699.07 (39.36)	0.033	0.219	0.219
NCGMV, ml	780.47 (76.20)	839.46 (59.41)	0.148	0.008	0.009
NDGMV, ml	58.80 (6.88)	65.08 (4.59)	0.207	0.001	0.002
NLV, ml	22.46 (15.99)	–	–	–	–
WM damage					
Whole brain average FA	0.33 (0.03)[a]	0.36 (0.02)	0.335	< 0.001	< 0.001
Severity score					
Average Z-score skeleton	−0.61 (0.50)[a]	0.00 (0.34)	0.321	< 0.001	< 0.001
Extent score					
Number of affected voxels (%)	3430.30 (5115.74)[a] (2.87%)	21.90 (55.86) (0.02%)	0.822	< 0.001	< 0.001

Displayed data are mean (standard deviation).
HCs = healthy controls; NCGMV = normalized cortical grey matter volume; NDGMV = normalized deep grey matter volume; NLV = normalized lesion volume; NWMV = normalized white matter volume; WM = white matter; p corr. = false discovery rate corrected p-values; pwMS = people with multiple sclerosis.
[a] n = 27.

working memory, and verbal fluency (see Table A.1). In total, 6 pwMS met the criteria for cognitive impairment (scoring at least 2 SD below that of HCs on at least 2 tests). Accuracy on the IPS task inside the scanner did not differ between groups.

3.2. Structural brain changes

NWMV was similar between groups (see Table 2), while pwMS displayed lower NCGMV (corr. $p = 0.009$) and NDGMV (corr. $p = 0.002$). The severity and extent of WM damage was worse in pwMS compared to HCs (corr. $p < 0.001$ for both). Furthermore, whole brain FA was lower in pwMS than in HCs (corr. $p < 0.001$).

3.3. Static and dynamic FC

No group differences were observed for RS and task-state sFC and dFC of the DMN (see Table 3). Additionally, in both groups ΔsFC-DMN did not differ significantly from zero (mean ΔsFC-DMN pwMS: -0.02 ± 0.06, $t(28) = 1.70$, corr. $p = 0.133$; mean ΔsFC-DMN HCs: -0.02 ± 0.07, $t(17) = 1.06$, corr. $p = 0.304$), suggesting no difference in sFC between RS and task-state. Furthermore, ΔsFC-DMN did not differ between pwMS and HCs.

In pwMS and HCs, ΔdFC-DMN differed significantly from zero (mean ΔdFC-DMN pwMS: 0.02 ± 0.02, $t(28) = 3.63$, corr. $p = 0.004$; mean ΔdFC-DMN HCs: 0.03 ± 0.01, $t(17) = 2.81$, corr. $p = 0.024$), suggesting an increase in dFC of the DMN during task-state relative to RS. No group differences in ΔdFC-DMN were observed.

3.4. Relationship between dFC and conventional brain measures

After correction for multiple testing, none of the correlation coefficients between dynamic and conventional brain measures were statistically significant in pwMS or HCs (corr. $p > 0.251$).

3.5. Predicting IPS

3.5.1. mSDMT accuracy

In pwMS, mSDMT accuracy inside the scanner could not be predicted by conventional brain measures (block 1–4; Table 4). However, when adding block 5, the model predicted 23% of the variance in mSDMT accuracy, effectively by ΔdFC-DMN only ($\beta = 0.51$, $p = 0.006$). In HCs, 23% of variance in mSDMT accuracy could be explained by RS dFC of the DMN only ($\beta = 0.53$, $p = 0.025$). For both pwMS and HCs, Fig. 2A displays the relationship between the final model and the outcome measure.

3.5.2. IPS composite Z-score

In pwMS, confounders and conventional brain measures could explain 26% of variance in IPS composite Z-score (block 1–4) with NCGMV ($\beta = 0.47$, $p = 0.050$) as predictor (Table 4). When adding dFC of the DMN, the amount of explained variance increased to 52% (R^2 change = 0.25, $p = 0.001$). The predictors now included NCGMV ($\beta = 0.49$, $p = 0.013$) and ΔdFC-DMN ($\beta = 0.52$, $p = 0.001$). In HCs, none of the predictors were significantly related to IPS outside the scanner. Fig. 2B displays the relationship between the final model and the outcome measure.

Table 3
Task-state and resting-state stationary and dynamic functional connectivity.

	pwMS (n = 29)	HCs (n = 18)	Effect size (η^2)	p	p corr.
Average head motion					
Resting-state (mm)	0.068 (0.035)	0.068 (0.028)	< 0.001	0.989	0.989
Task-state (mm)	0.091 (0.042)	0.068 (0.036)	0.075	0.063	0.167
Resting-state					
sFC DMN	0.959 (0.051)	0.952 (0.052)	0.005	0.647	0.989
dFC DMN	1.018 (0.030)	1.019 (0.024)	< 0.001	0.8933	0.989
Task-state					
sFC DMN	0.940 (0.048)	0.935 (0.040)	< 0.001	0.957	0.989
dFC DMN	1.034 (0.024)	1.049 (0.027)	0.035	0.213	0.167
Difference					
Task-state minus resting-state					
ΔsFC-DMN	−0.019 (0.060)	−0.017 (0.068)	< 0.001	0.917	0.989
ΔdFC-DMN	0.016 (0.023)	0.029 (0.044)	0.042	0.168	0.167

Displayed data are mean (standard deviation).
dFC = dynamic functional connectivity; DMN = default mode network; HCs = healthy controls; p corr. = false discovery rate corrected p-values; pwMS = people with multiple sclerosis; sFC = stationary functional connectivity.

Table 4
Hierarchical regression models for predicting mSDMT performance and IPS composite *Z*-score.

			Adjusted R^2	Standardized β	Test statistic	*p*
mSDMT accuracy	pwMS	Full model: block 1–4	N/A		N/A	N/A
		Full model: block 1–5	0.23		8.83[a]	0.006
		ΔdFC-DMN		0.51	2.97[b]	0.006
	HCs	Full model: block 1–4	N/A		N/A	N/A
		Full model: block 1–5	0.23		6.10[a]	0.025
		RS dFC-DMN		−0.53	−2.47[b]	0.025
IPS composite *Z*-score	pwMS	Full model: block 1–4	0.26		5.65[a]	0.010
		Age		−0.14	−0.60[b]	0.554
		NCGMV		0.47	2.07[b]	0.050
		Full model: block 1–5	0.52		10.20[a]	< 0.001
		Age		< 0.01	< 0.01[b]	0.998
		NCGMV		0.49	2.69[b]	0.013
		ΔdFC-DMN		0.52	3.67[b]	0.001
	HCs	Full model: block 1–4	N/A		N/A	N/A
		Full model: block 1–5	N/A		N/A	N/A

dFC = dynamic functional connectivity; DMN = default mode network; HCs = healthy controls; IPS = information processing speed; mSDMT = modified Symbol Digit Modalities Test; N/A = not applicable; pwMS = people with multiple sclerosis; RS = resting-state; sFC = stationary functional connectivity.
[a] *F*-value.
[b] *t*-value.

3.6. Post hoc specificity analysis

Within both groups, no significant relationship was found between ΔdFC-DMN and EDSS score (MS: corr. $p = 0.860$), fatigue (MS: corr. $p = 0.768$; HC: corr. $p = 0.712$), depression (MS and HCs: corr. $p = 0.712$) or any neuropsychological test (MS and HCs corr. $p > 0.712$).

3.7. Post hoc exploration: Effect of switching medication

No differences were found between switchers ($n = 13$) and non-switchers ($n = 19$) with respect to demographics, disease characteristics, IPS composite *Z*-score, or mSDMT accuracy (Table A.2). Furthermore, no significant group differences were found regarding structural MRI, sFC and dFC of the DMN.

No effect of switching was found on mSDMT accuracy (β = −0.14, $p = 0.395$). Furthermore, adding the interaction between switching with ΔdFC-DMN to the model did not increase the amount of explained variance (R^2 change = 0.02, $p = 0.463$), resulting in a final model explaining 23% of variance in mSDMT by ΔdFC-DMN (β = 0.52, $p = 0.005$). Similar findings were obtained for IPS composite *Z*-score: no effect of switchers/non-switchers was found on this dependent

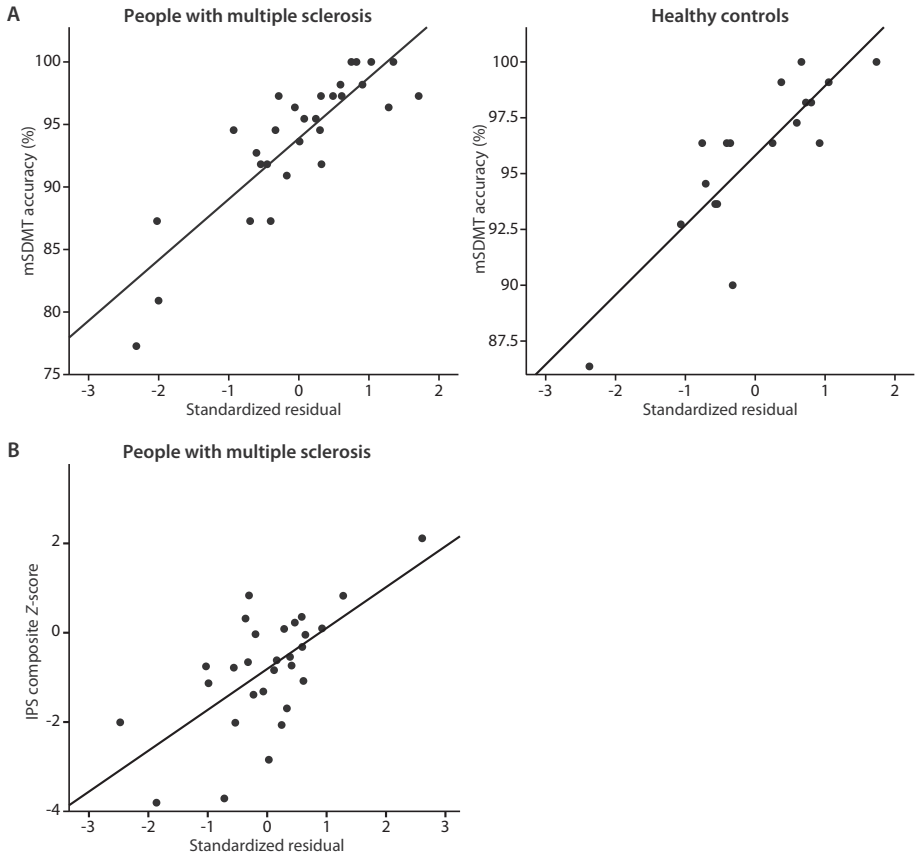

Fig. 2. Relationship between the regression model and outcome measures
For both accuracy on the modified symbol digit modalities test (A) and information processing speed composite *Z*-score (B), the standardized residuals of the final regression model, including dynamic functional connectivity of the default mode network, is plotted against performance for people with MS and healthy controls separately.
IPS = information processing speed; mSDMT = modified Symbol Digit Modalities Test.

variable ($\beta = -0.16$, $p = 0.263$). Additionally, adding the interaction terms between switchers/non-switchers with ΔdFC-DMN and NCGMV did not improve the model in terms of explained variance (R^2 change = 0.04, $p = 0.358$). In total, 54% of variance could be explained by NCGMV ($\beta = 0.44$, $p = 0.004$) and ΔdFC-DMN ($\beta = 0.53$, $p < 0.001$).

4. Discussion

In the present study, we investigated the incremental value of dFC of the DMN over conventional measures of brain abnormalities in explaining IPS in MS. In pwMS, an increase in dFC of the DMN from RS to task-state (i.e. ΔdFC-DMN) was a relevant predictor for better IPS inside the scanner (i.e. task accuracy) and outside the scanner (IPS composite *Z*-score). In the latter case, adding dFC of the DMN to the regression model, on top of conventional brain measures, doubled the amount of explained variance to a total of 52% (with NCGMV as another significant predictor). These results suggest that the DMN might alter its dFC pattern upon task demands, which we refer to as "DMN responsivity". Furthermore, our results suggest that in MS, individual differences in DMN responsivity can be related to individual differences in IPS.

4.1. Conventional MRI and IPS

Problems with IPS in MS have typically been explained as a consequence of WM damage, such as lesions and decreased integrity, but also of cortical and deep GM atrophy (Randolph et al., 2005; Mazerolle et al., 2013; Batista et al., 2012). Although WM damage or deep GM atrophy were not identified as the most important predictors for IPS in our sample, we did observe that NCGMV could explain up to 26% of variance in IPS outside the scanner. With respect to sFC, we did not observe differences between pwMS and controls, whereas previous studies did show differences in DMN effective and stationary FC at rest and during an IPS task, both related to IPS (Dobryakova et al., 2016; Wojtowicz et al., 2014). These contradictory findings might be explained by methodological differences, such as sample size and operationalization of FC. With respect to the latter, a previous study used a seed-based approach instead of an atlas-based approach on RS data only (Wojtowicz et al., 2014). The other study investigated the *directionality* of FC (i.e. effective FC) during IPS, which provides differential information than sFC, and is therefore difficult to compare (Dobryakova et al., 2016). Furthermore, we normalized FC measures for whole-brain average FC, as this average FC can vary greatly between subjects and potentially drive differences between groups, which is not always performed in other studies. Applying this normalization step allowed us to deal with individual differences in FC, and can thereby more accurately reflect possible changes in FC between groups.

4.2. Dynamics and IPS

Although no differences between pwMS and HCs were observed between dFC of the DMN, adding dFC to the regression model, next to confounding variables and conventional MRI measures, increased the explained variance by the model for IPS inside and outside the scanner. Furthermore, we did not observe a significant relationship between ΔdFC-DMN and EDSS score, fatigue, depression or any other neuropsychological test score, suggesting that our findings are specific for IPS. Changes in RS DMN dynamics have been observed in other neurological disorders, including schizophrenia, autism, attention deficit hyperactivity disorder, depression, and epilepsy. Often, these changes were related to the severity of symptoms (Zhang et al., 2016; Sambataro et al., 2017; Douw et al., 2015; Liu et al., 2017). A large challenge to directly compare between study results is differences in operationalization of DMN dynamics (e.g. standard deviation of FC, non-overlapping windows, or spectrum analysis) but also variation in types of pathology. Nevertheless, the present measure of dFC was able to pick up individual differences in pwMS and HCs regarding dFC of the DMN and IPS. This is in line with a recent study that was able to identify individuals based on spatial patterns of dynamic characteristics of FC (i.e. 'fingerprinting'), which was a significant predictor for higher order cognitive functions (i.e. fluid intelligence and executive functions) (Liu et al., 2018).

4.3. DMN responsivity

In both pwMS and HCs, an increase in dFC of the DMN was observed from RS to task-state, suggesting that this might be a response upon increasing cognitive demands. Interestingly, a larger increase in dFC from RS to task-state in pwMS was the only significant predictor for IPS inside the scanner, as well as a significant predictor for IPS outside the scanner (next to NCGMV). These findings suggest that during IPS, the DMN seems to change its FC pattern more often than during RS, possibly reflecting increased information flow throughout the network (Vatansever et al., 2015b). In HCs, however, lower RS dFC of the DMN was related to better IPS inside the scanner, whereas no predictors were found for IPS outside the scanner (probably explained by limited variation in performance and obtained brain measures). Previous studies in healthy subjects have linked both lower and higher brain dynamics during RS to better cognitive functioning (Jia et al., 2014; Douw et al., 2016; Nomi et al., 2017). These varying results illustrate the complexity of both brain dynamics and human cognition, their relationship in health and neurological disorders, and the relative infancy of this field of research.

The behavioral relevance of increasing DMN dynamics during task-state relative to RS is in line with a previous study in healthy subjects on cognitive flexibility (i.e. Stroop task) and dFC of the DMN with the frontoparietal network (Douw et al., 2016). That is, higher dFC of the DMN with frontoparietal network during task-state and lower dFC during RS in isolation were related to better cognitive flexibility outside the scanner (Douw et al., 2016). However, a larger increase in task-state relative to RS dFC explained even more variance in cognitive flexibility (Douw et al., 2016). Another study found that the frontoparietal network was more dynamic during working memory compared to a control condition, which could be related to better working memory and executive functions (Braun et al., 2015). For sFC, the increase in DMN connectivity with respect to increasing task-load has been described previously in healthy subjects (Elton and Gao, 2015; Vatansever et al., 2015a). In turn, this DMN responsivity could be related to maintained task performance (Elton and Gao, 2015; Vatansever et al., 2015a). Metaphorically, this task-evoked responsivity of the brain might be similar as performing a challenging physical exercise that exposes certain cardiac conditions (Gonzalez-Castillo and Bandettini, 2017). Hence, one could speculate that combining RS with task-state functional measures might (partly) capture the ability of a patient's functional network to adapt upon task demands, which might explain a patient's cognitive abilities (Gonzalez-Castillo and Bandettini, 2017).

4.4. Switching medication

The present MS sample consisted of pwMS switching to fingolimod treatment and non-switchers continuing with first-line therapy. The status of pwMS (switchers/non-switchers) did not relate to IPS or mediated the relationship between ΔdFC-DMN and NCGMV with IPS. These findings suggest that switchers were statistically similar to non-switchers. However, one should keep in mind that more than half of the switchers used first-line therapy prior to fingolimod and changed therapy because of disease activity ($n = 7$), whereas positivity for John Cunningham virus, and therefore at risk for developing progressive multifocal leukoencephalopathy, was the main reason for pwMS to switch from natalizumab to fingolimod ($n = 6$) and not so much disease activity. Future studies should explore possible changes in brain dynamics under MS treatment over time in relationship to disease activity

and cognitive functioning.

The first limitation of the present study is the small sample size that limits the statistical power. This might explain why we did not observe group differences in sFC and dFC, which could be a Type II error. Furthermore, although we included various explanatory variables in the regression analysis, we made a preselection of predictors and focused on the most relevant variables by using a forward selection procedure. Secondly, unfortunately we did not measure premorbid IQ, which might more accurately reflect premorbid cognitive functioning than educational level. Thirdly, as negative correlation coefficients for sFC and dFC could make correction for whole-brain sFC/dFC and comparisons between RS and task-state conditions challenging (i.e. dividing by a negative value), we decided to calculate absolute connectivity values. Finally, the difference measure between task-state and RS sFC/dFC should be interpreted with some caution, as both fMRI sequences were slightly different in terms of scanning parameters (e.g. TR). This resulted in subtle differences in window length for dFC (0.6 s) and shift (1 s). However, these differences are marginal, and by normalizing for whole-brain sFC/dFC we believe the effects of different scanning parameters on our results is minimal.

4.5. Future perspective

In the present study, we specifically focused on dFC of the DMN, based on previous studies showing changes in the DMN in MS, its relevance for cognition, and to limit the number of statistical tests with respect to sample size (Raichle, 2015; Rocca et al., 2010). Hence, one should keep in mind that we only investigated part of the story regarding the link between brain dynamics and IPS. As a next step in MS, future studies in larger samples should investigate dynamics of all brain networks during RS and task-state (and the responsivity), and link this to other cognitive domains. Furthermore, future studies should increase their sample size and the duration of fMRI sequences in order to test the reliability of findings (e.g. with a split-half analysis).

4.6. Conclusions

In conclusion, on top of conventional brain measures, higher dFC of the DMN during task-state relative to RS was an important predictor for IPS in MS in this study. These findings could reflect the ability of the DMN to adapt its dFC pattern upon task demands, in order to maintain optimal IPS. Future studies should investigate brain dynamics and IPS over time, as well as the generalizability of our findings to dynamics of other brain networks and cognitive domains.

Disclosures

This study was funded by Novartis.

Q. van Geest receives research support from Novartis.

L. Douw receives research support from a Branco Weiss Fellowship from Society in Science.

S. van't Klooster reports no disclosures.

C.E. Leurs receives research support from the Dutch MS Research Foundation.

H.M. Genova reports no disclosures.

G.R. Wylie reports no disclosures.

M.D. Steenwijk reports no disclosures.

J. Killestein accepted speaker and consulting fees from Merck Serono, Biogen, TEVA, Genzyme, Roche and Novartis.

J.J.G. Geurts serves on the editorial boards of MS Journal, BMC Neurology, MS International and Neurology, and has served as a consultant for Merck-Serono, Biogen Idec, Novartis, Sanofi-Genzyme and Teva Pharmaceuticals.

H.E. Hulst receives research support from the Dutch MS Research Foundation, grant number 08–648 and serves as a consultant for Genzyme and Merck-Serono.

Appendix A. Supplementary data

Supplementary data to this article can be found online at https://doi.org/10.1016/j.nicl.2018.05.015.

References

Amato, M.P., Portaccio, E., Goretti, B., et al., 2010. Cognitive impairment in early stages of multiple sclerosis. Neurol. Sci. 31, S211–214.

Andersson, J.L., Skare, S., Ashburner, J., 2003. How to correct susceptibility distortions in spin-echo echo-planar images: application to diffusion tensor imaging. NeuroImage 20, 870–888.

Batista, S., Zivadinov, R., Hoogs, M., et al., 2012. Basal ganglia, thalamus and neocortical atrophy predicting slowed cognitive processing in multiple sclerosis. J. Neurol. 259, 139–146.

Benedict, R.H., Cookfair, D., Gavett, R., et al., 2006. Validity of the minimal assessment of cognitive function in multiple sclerosis (MACFIMS). J. Int. Neuropsychol. Soc. 12, 549–558.

Benjamini, Y., Hochberg, Y., 1995. Controlling the false discovery rate: a practical and powerful approach to multiple testing. J. R. Stat. Soc. 57, 289–300.

Braun, U., Schafer, A., Walter, H., et al., 2015. Dynamic reconfiguration of frontal brain networks during executive cognition in humans. Proc. Natl. Acad. Sci. U. S. A. 112, 11678–11683.

Chard, D.T., Jackson, J.S., Miller, D.H., Wheeler-Kingshott, C.A., 2010. Reducing the impact of white matter lesions on automated measures of brain gray and white matter volumes. J. Magn. Reson. Imaging 32, 223–228.

Chiaravalloti, N.D., DeLuca, J., 2008. Cognitive impairment in multiple sclerosis. Lancet Neurol. 7, 1139–1151.

Cohen, J.R., 2017. The behavioral and cognitive relevance of time-varying, dynamic changes in functional connectivity. NeuroImage. http://dx.doi.org/10.1016/j.neuroimage.2017.09.036. (Epub ahead of print).

Cole, M.W., Ito, T., Bassett, D.S., Schultz, D.H., 2016. Activity flow over resting-state networks shapes cognitive task activations. Nat. Neurosci. 19, 1718–1726.

De, Hammes J., 1973. Stroop Kleur-Woord Test: Handleiding. Swets & Zeitlinger, Amsterdam.

Dobryakova, E., Costa, S.L., Wylie, G.R., DeLuca, J., Genova, H.M., 2016. Altered effective connectivity during a processing speed task in individuals with multiple sclerosis. J. Int. Neuropsychol. Soc. 22, 216–224.

Douw, L., Leveroni, C.L., Tanaka, N., et al., 2015. Loss of resting-state posterior cingulate flexibility is associated with memory disturbance in left temporal lobe epilepsy. PLoS One 10, e0131209.

Douw, L., Wakeman, D.G., Tanaka, N., Liu, H.S., Stufflebeam, S.M., 2016. State-dependent variability of dynamic functional connectivity between frontoparietal and default networks relates to cognitive flexibility. Neuroscience 339, 12–21.

Elton, A., Gao, W., 2015. Task-positive functional connectivity of the default mode network transcends task domain. J. Cogn. Neurosci. 27, 2369–2381.

Fan, L.Z., Li, H., Zhuo, J.J., et al., 2016. The human Brainnetome atlas: a new brain atlas based on connectional architecture. Cereb. Cortex 26, 3508–3526.

van Geest, Q., Hulst, H.E., Meijer, K.A., Hoyng, L., JJG, Geurts, Douw, L., 2018. The importance of hippocampal dynamic connectivity in explaining memory function in multiple sclerosis. Brain Behav. http://dx.doi.org/10.1002/brb3.954. (Epub ahead of print).

Genova, H.M., Hillary, F.G., Wylie, G., Rypma, B., Deluca, J., 2009. Examination of processing speed deficits in multiple sclerosis using functional magnetic resonance imaging. J. Int. Neuropsychol. Soc. 15, 383–393.

Glanz, B.I., Healy, B.C., Rintell, D.J., Jaffin, S.K., Bakshi, R., Weiner, H.L., 2010. The association between cognitive impairment and quality of life in patients with early multiple sclerosis. J. Neurol. Sci. 290, 75–79.

Gonzalez-Castillo, J., Bandettini, P.A., 2017. Task-based dynamic functional connectivity: recent findings and open questions. NeuroImage. http://dx.doi.org/10.1016/j.neuroimage.2017.08.006. (Epub ahead of print).

Ito, T., Kulkarni, K.R., Schultz, D.H., et al., 2017. Cognitive task information is transferred between brain regions via resting-state network topology. Nat. Commun. 8, 1027.

Jia, H., Hu, X., Deshpande, G., 2014. Behavioral relevance of the dynamics of the functional brain connectome. Brain Connect. 4, 741–759.

Jolles, J., Houx, P.J., van Boxtel, M.P.J., Ponds, R.W.H.M., 1995. Maastricht Aging Study: Determinants of Cognitive Aging. Neuropsychological Publishers, Maastricht, The Netherlands.

Kurtzke, J.F., 1983. Rating neurologic impairment in multiple-sclerosis - an expanded disability status scale (Edss). Neurology 33, 1444–1452.

Leonardi, N., Van De Ville, D., 2015. On spurious and real fluctuations of dynamic functional connectivity during rest (vol 104, pg 430, 2015). NeuroImage 104, 464–465.

Lin, P., Yang, Y., Gao, J., et al., 2017. Dynamic default mode network across different brain states. Sci. Rep. 7, 46088.

Liu, F., Wang, Y.F., Li, M.L., et al., 2017. Dynamic functional network connectivity in idiopathic generalized epilepsy with generalized tonic-clonic seizure. Hum. Brain Mapp. 38, 957–973.

Liu, J., Liao, X., Xia, M., He, Y., 2018. Chronnectome fingerprinting: identifying individuals and predicting higher cognitive functions using dynamic brain connectivity patterns. Hum. Brain Mapp. 39, 902–915.

Mazerolle, E.L., Wojtowicz, M.A., Omisade, A., Fisk, J.D., 2013. Intra-individual variability in information processing speed reflects white matter microstructure in multiple sclerosis. Neuroimaging Clin. 2, 894–902.

Nomi, J.S., Vij, S.G., Dajani, D.R., et al., 2017. Chronnectomic patterns and neural flexibility underlie executive function. NeuroImage 147, 861–871.
Raichle, M.E., 2015. The brain's default mode network. Annu. Rev. Neurosci. 38, 433–447.
Randolph, J.J., Wishart, H.A., Saykin, A.J., et al., 2005. FLAIR lesion volume in multiple sclerosis: relation to processing speed and verbal memory. J. Int. Neuropsychol. Soc. 11, 205–209.
Rocca, M.A., Valsasina, P., Absinta, M., et al., 2010. Default-mode network dysfunction and cognitive impairment in progressive MS. Neurology 74, 1252–1259.
Sambataro, F., Visintin, E., Doerig, N., et al., 2017. Altered dynamics of brain connectivity in major depressive disorder at-rest and during task performance. Psychiatry Res. Neuroimaging 259, 1–9.
Schoonheim, M.M., Vigeveno, R.M., Rueda Lopes, F.C., et al., 2014. Sex-specific extent and severity of white matter damage in multiple sclerosis: implications for cognitive decline. Hum. Brain Mapp. 35, 2348–2358.
Shine, J.M., Bissett, P.G., Bell, P.T., et al., 2016. The dynamics of functional brain networks: integrated network states during cognitive task performance. Neuron 92, 544–554.
Simony, E., Honey, C.J., Chen, J., et al., 2016. Dynamic reconfiguration of the default mode network during narrative comprehension. Nat. Commun. 7, 12141.
Smith, S.M., Zhang, Y., Jenkinson, M., et al., 2002. Accurate, robust, and automated longitudinal and cross-sectional brain change analysis. NeuroImage 17, 479–489.
Smith, S.M., Jenkinson, M., Johansen-Berg, H., et al., 2006. Tract-based spatial statistics: voxelwise analysis of multi-subject diffusion data. NeuroImage 31, 1487–1505.
Steenwijk, M.D., Pouwels, P.J., Daams, M., et al., 2013. Accurate white matter lesion segmentation by k nearest neighbor classification with tissue type priors (kNN-TTPs). Neuroimaging Clin. 3, 462–469.
Vatansever, D., Menon, D.K., Manktelow, A.E., Sahakian, B.J., Stamatakis, E.A., 2015a. Default mode network connectivity during task execution. NeuroImage 122, 96–104.
Vatansever, D., Menon, D.K., Manktelow, A.E., Sahakian, B.J., Stamatakis, E.A., 2015b. Default mode dynamics for global functional integration. J. Neurosci. 35, 15254–15262.
Vercoulen, J.H., Swanink, C.M., Fennis, J.F., Galama, J.M., van der Meer, J.W., Bleijenberg, G., 1994. Dimensional assessment of chronic fatigue syndrome. J. Psychosom. Res. 38, 383–392.
Wojtowicz, M., Mazerolle, E.L., Bhan, V., Fisk, J.D., 2014. Altered functional connectivity and performance variability in relapsing-remitting multiple sclerosis. Mult. Scler. 20, 1453–1463.
Xie, H., Calhoun, V.D., Gonzalez-Castillo, J., et al., 2017. Whole-brain connectivity dynamics reflect both task-specific and individual-specific modulation: a multitask study. NeuroImage. http://dx.doi.org/10.1016/j.neuroimage.2017.05.050. (Epub ahead of print).
Yang, Z., Craddock, R.C., Margulies, D.S., Yan, C.G., Milham, M.P., 2014. Common intrinsic connectivity states among posteromedial cortex subdivisions: insights from analysis of temporal dynamics. NeuroImage 93 (Pt 1), 124–137.
Yeo, B.T.T., Krienen, F.M., Sepulcre, J., et al., 2011. The organization of the human cerebral cortex estimated by intrinsic functional connectivity. J. Neurophysiol. 106, 1125–1165.
Zhang, J., Cheng, W., Liu, Z.W., et al., 2016. Neural, electrophysiological and anatomical basis of brain-network variability and its characteristic changes in mental disorders. Brain 139, 2307–2321.
Zigmond, A.S., Snaith, R.P., 1983. The hospital anxiety and depression scale. Acta Psychiatr. Scand. 67, 361–370.